Development of a Low-Cost Loudspeaker-Driven Thermoacoustic Refrigerator

Luke Zoontjens, Carl Q. Howard, Anthony C. Zander and Ben S. Cazzolato

School of Mechanical Engineering, The University of Adelaide, Australia

ABSTRACT

Thermoacoustic refrigeration is an emerging 'green' technology based upon the purposeful use of high-pressure sound waves to provide cooling. This paper describes the development of a thermoacoustic refrigerator built with the aim of using domestic 'off the shelf' parts where possible. The key considerations and tools used in the design and development of the thermoacoustic refrigerator are discussed, and results detailing the performance of the device obtained from direct measurements and computer modelling are compared.

INTRODUCTION

Thermoacoustic refrigeration is an emerging 'green' technology based upon the purposeful use of high-pressure sound waves to provide cooling. Thermoacoustic devices require no environmentally harmful refrigerants or lubricants, and are inexpensive to manufacture compared to vapour compression refrigeration systems.

Thermoacoustic systems are generally divided into two classes: 'heat engines' (also known as 'prime movers'), which convert heat from temperature differentials into acoustic power, and 'heat pumps', which consume acoustic power to transport or 'pump' heat. Thermoacoustic heat engines can also be coupled to heat pumps, such that heat converted into acoustic power by the heat engine is utilised by the heat pump to provide cooling. Where a heat pump is driven by a heat engine or other acoustic source (such as a loudspeaker or commercial driver), the overall system is termed a 'refrigerator'.

Although arguably only in mainstream development for the last 25 years (Rott 1980), thermoacoustic systems are highly capable devices with wide ranging applications: from electricity generation to liquefaction of natural gas (Wollan and Swift 2002), and from cooling of electronics racks in US Naval warships to uses onboard the Space Shuttle Discovery (Garrett and Backhaus 2000).

Despite a recent increase in research interest into thermoacoustic systems, little information is available regarding the approach to the design and development of thermoacoustic refrigeration systems.

This paper will briefly outline the processes and resources involved in the design and manufacture of a loudspeaker-driven thermoacoustic refrigerator and discuss several key design aspects to consider. The main principles upon which thermoacoustic refrigerators operate are concisely detailed elsewhere (Swift 1988, 2002, Garrett 2004). Simple computer modelling and experimental techniques are also discussed.

DESIGN METHODOLOGY

Design of a thermoacoustic system starts with definition of its intended capability and purpose. Because the geometry and construction of a thermoacoustic device is strongly coupled to the thermodynamic conditions under which it operates, design of a thermoacoustic refrigerator is largely theoretical in the absence of experience or even empirical data to provide design cues.

Design and optimisation of loudspeaker-driven thermoacoustic refrigerators is well covered by Tijani *et al.* (2002a, 2002b) and also Wetzel and Herman (1997). Further to these, the following comments are added for the design of low-cost thermoacoustic systems.

Waveform configuration

The waveform configuration of the thermoacoustic device is an important early decision. Since thermoacoustic systems require high acoustic pressure amplitudes for useful operation, they are built such that the acoustic waves reinforce each other at the frequency of operation, i.e., they are driven at an acoustic resonance. Initial thermoacoustic devices were 'standing wave' designs, whereby the acoustic waves reflected from each end of a closed tube formed a standing wave inside the tube. The development of more efficient travelling wave systems (Backhaus and Swift 2000, Ueda *et al.* 2004, Sun *et al.* 2005) and 'cascade' systems (Backhaus and Swift 2002, Gardner and Swift 2003) which use a combination of standing and travelling wave system components, is an exciting area of thermoacoustics. These are, however, outside the scope of this paper due to the relative complexity associated with their design and manufacture.

Standing wave devices are further divided into 'half-wavelength' and 'quarter-wavelength' designs. A half-wavelength design operates at a frequency corresponding to a wavelength approximately twice the length of the closed tube. A quarter-wavelength design, such as that shown in Figure 1, has an effectively open termination at one end of the tube, which results in an operating frequency corresponding to a wavelength approximately four times the length of the tube. To contain the working fluid and prevent sound directly radiating to the environment, a buffer volume is added to the open termination. The quarter-wavelength design is considered more efficient since it presents less 'working wall area' for a given operating frequency – this reduces viscous losses from oscillating gas scrubbing along the walls. It should be noted that the wavelength dimensions are approximate, since local temperature gradients established by the device alter the resonant frequency of the internal fluid.

Energy sources

Thermoacoustic refrigerators are versatile in that the acoustic power used to drive them may originate from an electroacoustic driver or a heat engine, which itself may be driven by electrical inputs or reclaimed waste heat from another thermal process.

Loudspeaker driven thermoacoustic devices are arguably the easiest form of thermoacoustic refrigeration to implement successfully, since there is direct control over the acoustic content delivered to the heat pump and hence can be 'switched off' or 'throttled' almost immediately if needed. For this reason a loudspeaker-driven thermoacoustic refrigerator is highly recommended for a first attempt at thermoacoustic refrigeration.

Figure 1 shows the general layout of the thermoacoustic refrigerator (TAR) constructed at the University of Adelaide, and shows the general nomenclature and arrangement for a loudspeaker-driven thermoacoustic refrigerator. Figure 2 shows a 3D section model of the device to further visualise its assembly.

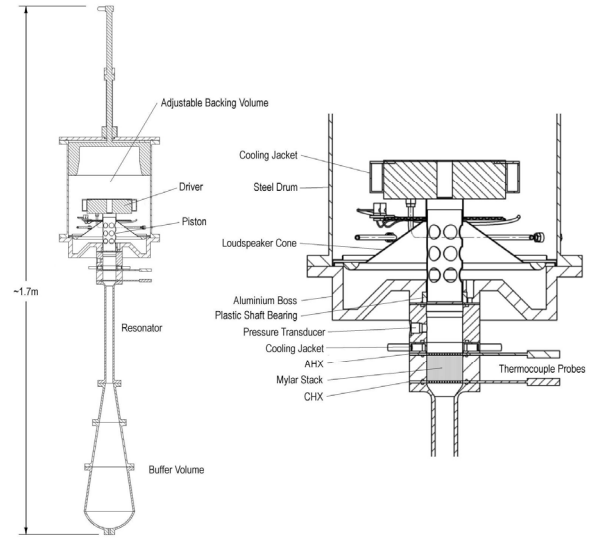

Figure 1. General layout of the loudspeaker-driven thermoacoustic refrigerator (TAR).

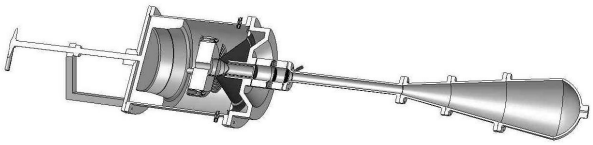

Figure 2. 3D section model of the 2003 TAR.

When the loudspeaker shown in Figure 1 is driven at the correct frequency and above a certain level, heat is drawn from the cold heat exchanger (CHX) and transported to the ambient heat exchanger (AHX). Water pumped through the cooling jacket carries heat away from the AHX.

Working Gas

Amongst the various qualities desired in a working gas, sound velocity and thermal conductivity are important. Since helium has the highest sound velocity and thermal conductivity of all inert gases (Tijani 2001), it makes for an excellent initial design choice; however for a low-cost thermoacoustic refrigerator, compressed air is a much less expensive option which can also be used to demonstrate the thermoacoustic cooling effect, albeit generally less efficiently.

Other thermoacoustic systems use helium-argon, helium-xenon or other noble-gas mixtures to improve efficiency, however the net benefit in achieving those efficiencies is questionable given the costs involved in obtaining, storing and mixing the gases.

Key Operation Parameters

Key design parameters in a thermoacoustic refrigerator are often considered to be the

- Cooling capacity, $\dot{Q}_c$, the rate of heat extraction at the CHX in Watts;
- Mean operating pressure, p_m;
- Mean temperature, T_m;
- Operating frequency f;
- Drive ratio, DR; and
- Temperature differential, ΔT, the difference in temperature between the AHX and the cold heat exchanger CHX in K.

The power density, and hence cooling capacity, in thermoacoustic devices can be increased by increasing the mean operating pressure and diameter (Swift 2002), however equal consideration should be given to safety precautions regarding the construction of the device, especially at high operating mean pressures.

The operating frequency is an important global parameter but is largely controlled by the internal shape of the device and the working fluid chosen. For the TAR shown in Figures 1 and 2, both helium and air were selected for operation - compressed air was used to develop the instrumentation and measurement procedures, with helium reserved for performance modelling and determining the actual cooling capacity of the device. The entire internal geometry of the TAR was based upon calculations using 700kPa helium (Arslanagic *et al.* 2003), however significant cooling effects have been demonstrated using 700kPa air in the device without alteration.

The drive ratio, DR, is defined as the ratio of the maximum acoustic pressure amplitude to the mean operating pressure:

$$DR = \frac{|p_A|}{p_m} \tag{1}$$

For reasonable modelling accuracy and to avoid severe non-linearities it is suggested that the drive ratio be kept below 3%, considered to be the limit for current thermoacoustic formulations (Poese and Garrett 2000).

The desired temperature differential is selected early for initial calculations, and iteratively adjusted to optimise the efficiency of the device.

SOME DESIGN ASPECTS

Further to the review by Swift (2002) of thermoacoustic design aspects, the following comments are provided to assist with the design of low-cost thermoacoustic systems.

Stacks

Stacks form the core of a thermoacoustic refrigerator and are in general designed first. Its properties are chosen iteratively

until a suitable compromise between the various performance characteristics is achieved.

Design of a low cost thermoacoustic refrigerator starts with placing constraints upon the stack material(s) and its geometry. For stacks proposed to be mass produced, Arnott *et al.* (1991) noted automotive ceramic substrates or monoliths to be an excellent choice. Readily available to the automotive industry for use in catalytic converters and particulate filters, ceramic substrates present a highly-desirable rectangular pore cross-section configuration, excellent cell rigidity, reasonable thermal conductivity, and wall thicknesses down to 0.064mm. Compared to stacks which are in part or entirely hand-assembled, the precision and consistency of ceramic substrate geometry is excellent.

For the TAR design described in this paper, a 36mm long parallel-plate stack constructed of 0.1mm Mylar sheeting spaced 0.45mm apart was previously constructed and is shown in Figure 3 (Arslanagic *et al.* 2003). Each Mylar sheet was hand-cut to the correct width according to its position in the circular section, and bonded with adhesive to 0.4mm x 0.5mm x 36mm polystyrene strips. The bonding agent was assumed to provide a spacing of 0.05mm, which enabled a spacing of 0.45mm (provided the 0.4mm 'side' of the polystyrene strip was used). The manufacturing methods used for this stack were highly labour intensive and not recommended for production of more than several stacks. Other stack manufacturing methods such as those for spiral stacks, pin arrays, and circular pore stacks are explained elsewhere (Swift 2002, Arslanagic *et al.* 2003), however all potentially suffer from geometrical inconsistencies from being hand-made.

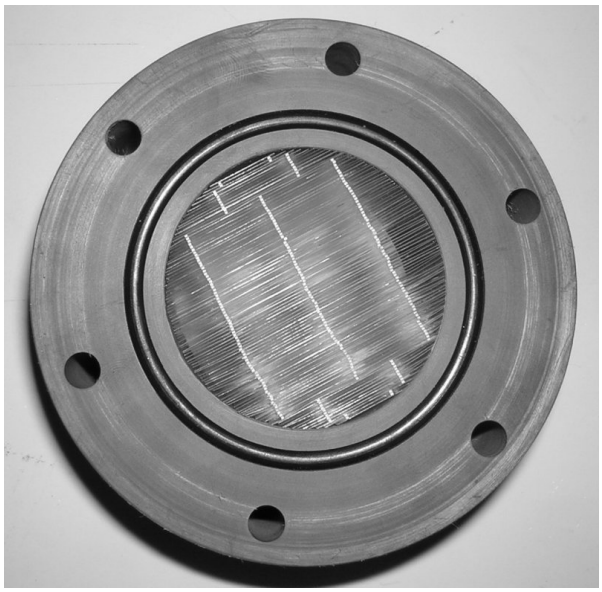

Source: (Arslanagic 2003)

Figure 3. Image of the actual TAR stack section. The columns of white polystyrene spacers in the Mylar stack can be clearly seen – the stack plates are arranged perpendicular to these. Note the black rubber 'O' ring used to seal the interfaces between the plastic stack collar and copper heat exchangers.

In comparison, a ceramic substrate can be easily sourced with 600 square 'cells' per square inch and a cell wall thickness of 0.11mm (4.3 thou). Ceramic substrates for the automotive emissions control industry are typically quoted in terms of cell density and wall thickness; the blockage ratio, *BR*, of square ceramic stacks can be found from

$$BR = CD\left(\frac{1}{\sqrt{CD}} - L_{wall}\right)^2 \quad (2)$$

where CD is the cell density (cells/m^2) and L_{wall} is the cell wall thickness (m). The relationship

$$BR = CD\left(\frac{1}{\sqrt{CD}} - \frac{L_{wall}}{1000}\right)^2 \quad (3)$$

is useful for when CD and L_{wall} are in typical cells per square inch (csi) and thou (thousandths of an inch) units respectively. The blockage ratio in Equations 2 and 3 is the ratio of open area in the pipe axis, and is used directly as an input in computer modelling regimes of thermoacoustic stacks.

Loudspeaker Drivers

Loudspeakers can be used effectively in a low-cost thermoacoustic refrigeration system; however several key aspects must be adhered to in order to extract the most performance from the loudspeaker.

The TAR described here is driven by a simple 12 inch diameter, 250W rated loudspeaker. This implementation of a large diameter loudspeaker from the outset of the design indirectly created problems with practicality and operation of the device. Incorporating the frame of the loudspeaker required a large support boss for mounting, and as can be seen in Figure 1, an aluminium piston attached to the voicecoil of the loudspeaker reached through this boss to present the driving face at the correct design location. The desired location for the driving face is shown in Figure 4 as the interface between the aluminium boss (B) and the pressure transducer boss (C).

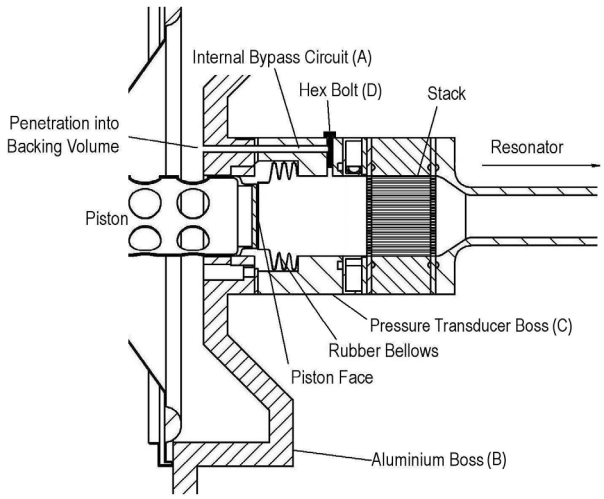

Figure 4. Detail of internal bypass circuit and rubber bellows for the TAR.

The central dust cap was removed from the loudspeaker to expose a 50mm collar, into which a hollow aluminium piston was inserted as a tight interference fit. Initially, as shown in Figure 1, the piston was sealed using a closely fitting circular plastic seal embedded into the aluminium boss.

Measurements showed that high pressure amplitudes developed at the face of the piston led to 'acoustic leakage' down the sides of the piston past the plastic seal. This leakage is believed to have dampened the acoustic mode of intended operation, degrading the quality factor of the acoustic

resonance. This effect has been noted by Mongeau *et al.* (2001).

To correct the problem, a rubber bellows was cut from an automotive CV joint boot seal and installed at the driving face of the piston (Figure 4). Whilst this action has largely improved the sealing of the piston, it is not ideal. Such an arrangement should be avoided, since pistons which reach inside the tube form sliding contacts which are difficult to effectively seal. Also, the increased mass of the long piston placed an additional load on the loudspeaker, reducing its electroacoustic efficiency. Instead, move the loudspeaker voice-coil or driver as close as possible to the desired driving position. Good examples of this are the arrangements of Tijani *et al.* (2002a) and Hofler (1986), which both use a suitable bellows to seal the driving face to the interior of the thermoacoustic system.

Pressure Equalisation (Bypass) Circuits

Typically, the electroacoustic driver and its backing volume are considered external to the thermoacoustic device interior; however these regions need to be kept at the same mean operating pressure as the thermoacoustic device. A gas bypass valve enables an equalisation of pressure across the piston face, however, if incorrectly executed, can affect the performance characteristics of the system.

For the section of the TAR shown in Figure 4, a gas bypass circuit (A) was drilled out of the aluminium boss (B) and extended almost to the end of the pressure transducer boss (C), where a tapped hole extended radially through the pressure transducer boss wall. A suitably sealed hex bolt (D) was installed into the tapped hole and wound in or out to allow a bypass of gas past the piston face as the device was pressurised. Without the hex bolt in place to block the bypass circuit, dynamic acoustic pressure would leak into the circuit and increase the effective damping of the system, reducing the quality factor of resonance.

An ideal method would be to use an external manifold system such as that shown in Figure 5, where an external pressure bypass circuit could link the two volumes upstream and downstream of the piston. Two valves should ideally be used; one valve at the driver end, as close as possible to the backing volume wall penetration, and the other located at the wall penetration, perhaps in the buffer volume where the acoustic velocity and pressure can be acceptably minimised. Locating the valves as close as possible to the interior of the device minimises the volume compliance formed by the column of gas extending from the interior to the valve face. Even small compliances such as these can dissipate a significant amount of precious acoustic power.

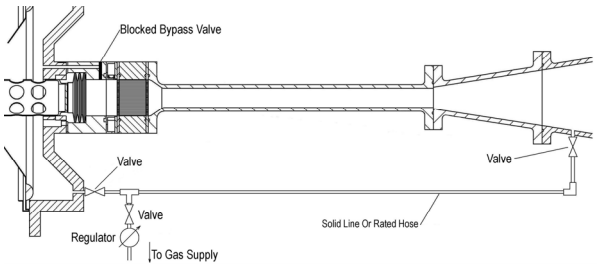

Figure 5. External manifolded bypass circuit for the TAR.

Sealing

Effective sealing is an important aspect in the design of thermoacoustic devices, and is given little attention in the literature. The problem of containing up to 20bars of fluid using simple materials is compounded by the small molecular size of helium and other light gas mixtures commonly used, which are often able to penetrate rubber seals and threaded connections. Furthermore, whilst mass-produced thermoacoustic refrigerators would theoretically never need to be opened or disassembled, laboratory versions are repeatedly disassembled and reconstructed to investigate various effects. The integration of good pressure seals which can be repeatedly broken into the design will result in improved and more predictable thermoacoustic performance, and cost savings in gas supply.

A popular method for construction of thermoacoustic systems is to use a modular approach, in which the stack, heat exchangers and resonator sections are all compressed together using a series of long bolts (Mongeau *et al.* 2001, Arslanagic *et al.* 2003). Whilst this construction is easy to disassemble, extreme care must be taken in the use of long bolts.

Consider the TAR design shown in Figures 1 and 2, where six M6 rods were used to sandwich the pressure transducer boss, cooling jacket, stack collar and both copper heat exchangers between the aluminium boss and the flange of the resonator section. Figure 3 also shows the 6.5mm diameter holes in the stack collar through which the M6 rods passed. The TAR was designed to contain 700kPa of helium, with minimal gas losses. However, the large volumes of pressurised gas at each end of the device (in the backing volume and the buffer volume termination) presented large axial surface areas which caused high tensile forces to be applied to the M6 rods. Small elastic strains in the rods led to gas escaping between the heat exchanger sections, despite the use of rubber 'O'-ring seals at every flange interface within the section. Although the use of high-tensile rods was found to curb the loss of gas to an acceptable level, it should be noted that the use of long steel rods to hold multiple sections together is not ideal. Several arrangements of flange sealing found to be effective are presented in Figure 6.

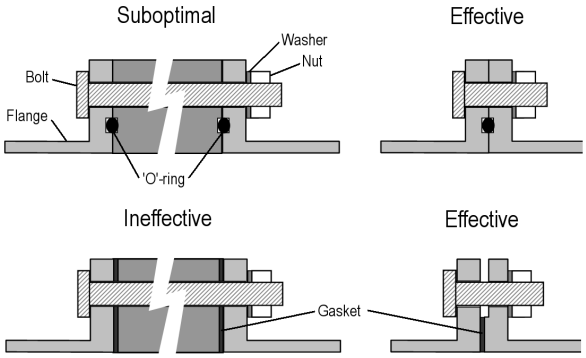

Figure 6. Typical flange connections for thermoacoustic pipe systems.

Flange connections with integral rubber or polymer 'O'-rings form a highly reliable connection, and have been used frequently in thermoacoustic devices (Swift 2002, Sun *et al.* 2005, Tang *et al.* 2005). A small step in the pipe wall could be used to hold stacks or components in place, in some instances removing the need for a flange connection altogether.

For laboratory devices, a useful alternative is to use a pressurised enclosure around sections or the entire apparatus (Tijani *et al.* 2002a, Gardner and Swift 2003). The pressurised enclosure is typically filled to a similar pressure as the internals of the thermoacoustic device, such that the net loading on the walls of the thermoacoustic device is reduced or eliminated. Also, reducing the axial surface area or

diameter of the device will reduce the tensile loading on flange connections.

Test Instrumentation

Mongeau *et al.* (2001) and Swift (1992, 2002) both detail effective measurement techniques for thermoacoustic systems. However, for preliminary work, pressure, acoustic velocity and temperature measurements are relatively simple to implement and can be used to estimate other important parameters. Figure 7 shows the arrangement and connection of test instrumentation for the TAR.

For the TAR, 'T' type thermocouples were inserted into machined slots in each copper heat exchanger such that they contacted the metal close to the internal volume. The output of each thermocouple was then sampled every 500ms by a data logger. A signal representing acoustic pressure was generated by an acoustic transducer close to the driving face of the piston (i.e. the pressure maximum) and amplified by an ICP power supply. A small accelerometer mounted on the inside face of the driving piston was used to measure the acceleration of the piston and hence estimate the volume velocity. The acceleration and acoustic pressure signals were sampled by an analyser which also was used to drive the loudspeaker via a 200W amplifier.

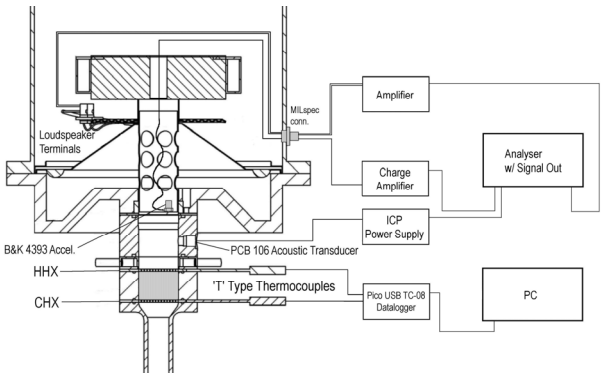

Figure 7. Simple layout diagram of test instrumentation used in the TAR.

Further to this instrumentation and as suggested by Swift (Swift 2002), thermocouples mounted at the inlet and outlet of the water cooling jacket, along with knowledge of the flowrate, enables reasonable estimation of the heat removed at the AHX, Q_H. Also, applying a constant heat load (e.g. via resistive heating elements) to the CHX under steady state conditions yields an estimate the cooling power of the device.

DeltaE Modelling

Dedicated computer aided design software for thermoacoustic systems is largely inexistent except for several programs developed by a number of educational and scientific organisations.

Of all the available thermoacoustic modelling programs, *DeltaE* (Ward and Swift 2001) is perhaps the most popular and effective. The DeltaE software, using linear thermoacoustic formulations, solves for 1-D complex pressure, volume velocity and temperature along the length of the thermoacoustic system. The suitable selection of 'guesses' and 'targets' is the key to successful use of the program: the program will iteratively adjust the variables listed as 'guesses' to achieve the 'target' values, e.g. a desired cooling power or temperature difference.

DeltaE was first used in the TAR design to identify the adiabatic (zero heat transfer) fundamental resonant frequency of the device and compare that with results obtained experimentally and also via an ANSYS modal analysis. The DeltaE resonant frequency was found by setting the pressure and volume velocity amplitudes low and reducing the energy transferred at the heat exchangers, such that the acoustic oscillations are as close to adiabatic as possible. The results of the comparison are given in Table 1.

For determination of the fundamental resonance frequency Table 1 indicates an accuracy of within 5% to that measured for both modelling programs. DeltaE considers only a one dimensional approach along the axis of the device, and the fluid elements used in ANSYS do not account for the acoustic impedances of the heat exchangers and stack which are present in the experimental measurement system. On this basis, here the estimates of both DeltaE and ANSYS are considered sufficiently accurate for design purposes. Knowledge of the resonant frequency of the device enabled more detailed modelling of the TAR.

Table 1. Fundamental resonance frequency of the TAR.

Quantity	DeltaE	ANSYS	Measured
f_{air}, Hz	113.6	118	119.2
f_{helium}, Hz	319.0	349	334.3

Experimental measurements were also performed using a 119.2Hz sinusoidal input, a working fluid of 700kPa air and a pressure amplitude of 15.3kPa as measured by an acoustic pressure transducer (shown in Figure 7) at approximately x=33mm. Under these conditions, the temperature difference between the AHX and CHX was measured during 25 minutes of operation, as shown in Figure 8. A maximum temperature difference of 15K was achieved between the two heat exchangers. The ambient temperature during the test was approximately 296K.

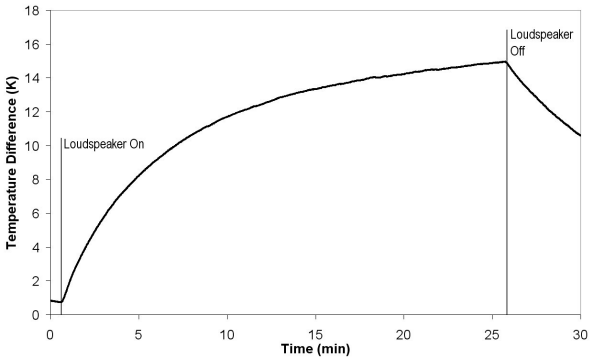

Figure 8. Measured TAR AHX/CHX temperature difference over time using 700kPa air.

It is believed that the time taken to achieve the 15K temperature difference was prolonged due to the materials used in the construction of the TAR. The copper CHX is compressed against the all-aluminium resonator section, which is exposed to ambient air. Insulating the CHX from the resonator section and ambient air would reduce the time taken to achieve steady state and most likely increase the temperature differential across the insulated stack.

Using this result, DeltaE was used to estimate the required internal state variables of the TAR, including the dynamic acoustic pressure amplitude $|p_A|$, to achieve a temperature difference of 15K between the AHX and the CHX as found experimentally.

This was achieved in DeltaE by the selection of guesses and targets as listed in Figure 9.

In DeltaE, the TAR is modelled in a series of segments which have various properties or parameters based upon their role in

the system. Address labels such as '0c' call the parameter 'c' in the segment '0'. Figure 9 shows the 'guesses' are all state variables for the position at the piston face; the initial temperature ('0c'), the dynamic pressure amplitude ('0d'), the phase between the acoustic pressure and volume velocity ('0e'), and the volume velocity ('0f'). DeltaE will adjust these four variables in an iterative process until the values for the 'targets' are achieved within acceptable tolerances. Figure 9 shows these targets are the temperatures at the AHX (Segment 5) and CHX (Segment 7), and the real and imaginary components of the inverse specific acoustic impedance at the buffer volume end of the TAR (Segment 13). The AHX and CHX temperature target values are set 15K apart, and to satisfy the boundary condition that the acoustic volume velocity is zero at the wall in the buffer volume, the inverse specific acoustic impedance targets are set to zero.

```
Iteration Vectors Summary:

 GUESS      0c          0d          0e          0f
 name  BEGIN:T-beg BEGIN: |p|  BEGIN:Ph(p) BEGIN: |U|
 units      K           Pa          deg        m^3/s
 value   305.53    -2.7302E+04 -2778.9      5.0821E-04
TARGET      5f          7f          13a         13b
 name  HXFRS:Est-T HXLAS:Est-T HARDE:R(1/z HARDE:I(1/z
 units      K           K
 value   303.00      288.00       0.0000      0.0000
result   303.00      288.00     2.6119E-07  3.9171E-07


Dependent Variables (outputs):
PLOTS       0A          0B          0C          0D          5G
            5H          7G          7H
 name  BEGIN:T-beg  BEGIN: |p|   BEGIN:Ph(p)  BEGIN: |U|   HXFRS:Heat
       HXFRS:Metal  HXLAS:Heat   HXLAS:Metal
 units      K           Pa          deg        m^3/s         W
            K           W           K
Independent Variables (inputs):
  Outer loop:   0b  BEGIN:Freq. Beg=  1.10E+02 End=  1.19E+02 Step=  5.00E-02
        181 points
```

Figure 9. Typical DeltaE Iteration Vectors Summary and Dependent Variable Plot Summary for the TAR.

Figure 9 includes the dependent variable plot summary used in the simulation. The value of address '0b', the operating frequency of the TAR, is here incremented in 0.05Hz steps from 110Hz to 119.2Hz. This means that for each operating frequency in the range given, the model is solved using the guesses to achieve the listed targets, and the results file generated will list the parameters specified in the plot summary against the operating frequency. This is a powerful tool in DeltaE: plotting the phase angle '0c' with frequency enables determination of the fundamental resonance frequency of the system (i.e. the frequency in which the initial phase angle is zero). Additional parameters and calculations via spreadsheet or DeltaE itself can estimate the frequency for optimal COP, COP_r, required acoustic pressure minimums, maximum cooling powers, or a wide variety of other key measures of performance. For our simulation, we chose to end the plot routine at 119.2Hz, such that the results of the calculation for the measured resonance frequency remain in the system cache. We then generated a plot of the state variables for that frequency, shown in Figure 10.

In Figure 10, the results of the DeltaE calculation are shown with regard to axial position along the axis of the TAR. DeltaE estimates the required maximum pressure amplitude to be approximately 27.3kPa, with around 0.8W of acoustic power consumed across the stack as it removes 4.1W of heat power from the CHX and delivers 5W of heat to the AHX. Note also that the program correctly minimises acoustic velocities at the ends of the device, and a pressure node / velocity antinode appears at the resonator termination (x=0.52m) as expected.

DeltaE's estimate of the pressure amplitude at the location of the acoustic pressure transducer, 27.2kPa (SPL ~180dB re 20μPa) is roughly 80% above the 15.3kPa (SPL ~175dB re 20μPa) measured, however when compared in terms of sound pressure level, a 5dB difference is considered reasonable in terms of modelling accuracy. Measurement of the state variables shown in Figure 10 at several locations along the axis of the device would facilitate a more accurate comparison with the simulated results.

The temperature distribution plot shown in Figure 10 also indicates another complexity in determining the ideal operating frequency of thermoacoustic devices. The resonant frequency measured experimentally shifts as sections of the TAR become colder: the volume of gas inside the TAR which becomes colder is larger than that which becomes warmer, so the overall resonant frequency shifts downward. Since the electroacoustic efficiency of the loudspeaker is best achieved at the fundamental resonance frequency, shifts in resonant frequency are undesirable. A possible solution is that suggested by Li *et al.* (2002) whereby the frequency at which the loudspeaker operates is actively 'tuned' to match the optimal frequency.

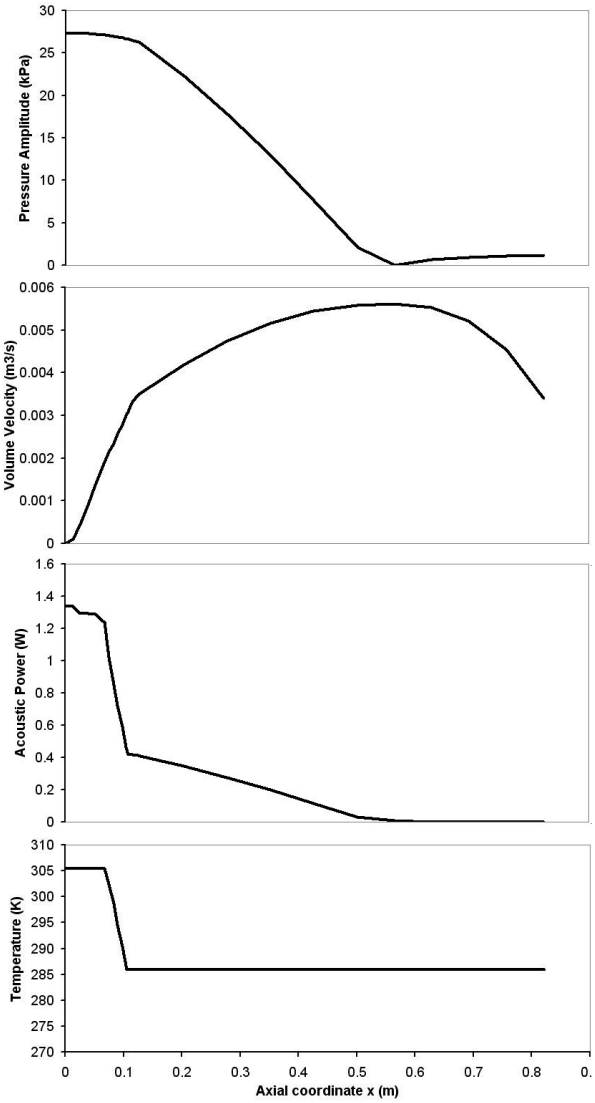

Figure 10. State variable plots from DeltaE for 700kPa air, an operating frequency of 119.2Hz and a cooling power of 5W.

The comparison between the predicted and experimentally measured results shows the ability for DeltaE to model the system performance with sufficient accuracy to enable the design and selection of various thermoacoustic systems and components for low-cost applications.

CONCLUSIONS

The approach to the design and manufacture of loudspeaker-driven thermoacoustic systems has been discussed with

consideration of low-cost technologies and simple measurement systems.

Details regarding the construction and modelling of a loudspeaker-driven thermoacoustic refrigerator at the University of Adelaide highlight typical issues involved in the development of such systems.

ACKNOWLEDGEMENTS

The authors would like to thank the Mazda Foundation for their generous support. The authors would also like to thank the administrative, technical and workshop staff at the School of Mechanical Engineering, University of Adelaide, for their assistance in many aspects of this work.

REFERENCES

Arnott, W.P., Bass, H.E., and Raspet, R. (1991) General formulation of thermoacoustics for stacks having arbitrarily shaped pore cross sections. *J. Acous. Soc. Am.* vol. 90, pp. 3228-3237.

Arslanagic, A., Brooks, L.A., and Li-Ying, E.C. (2003). *Thermoacoustic Refrigerator*. Level 4 Project Report, School of Mechanical Engineering, The University of Adelaide, Australia.

Backhaus, S.N., and Swift, G.W. (2000) A thermoacoustic Stirling heat engine: Detailed study. *J. Acoust. Soc. Am.* vol. 107, pp. 3148-3166.

Backhaus, S.N., and Swift, G.W. (2002) New Varieties of Thermoacoustic Engines. *Proceedings of the Ninth International Congress on Sound and Vibration*, Orlando FL, USA, July 8-11, vol. 502.

Gardner, D.L., and Swift, G.W. (2003) 'A cascade thermoacoustic engine', *J. Acoust. Soc. Am.* vol. 11, pp. 1905-1919.

Garrett, S.L. (2004) 'Resource letter: TA -1: Thermoacoustic engines and refrigerators', *Am. J. Phys.* vol. 72, no. 1: pp. 11-17.

Garrett, S.L., and Backhaus, S. (2000) 'The Power of Sound', *American Scientist*, vol. 88, no. 6.

Hofler, T.J. (1986) *Thermoacoustic refrigerator design and performance*, PhD Thesis, Physics Department, University of California, San Diego.

Li, Y., Minner, B.L., Chiu, G.T.C., Mongeau, L., and Braun, J.E. (2002) 'Adaptive tuning of an electrodynamically driven thermoacoustic cooler', *J. Acoust. Soc. Am.* vol. 111, pp. 1251-1258.

Mongeau, L., Alexander, A., Minner, B., Paek, I., and Braun, J.E. (2001) 'Experimental investigations of an electro-dynamically driven thermoacoustic cooler', *International Mechanical Engineering Congress and Exposition*, New York, NY pp. 1-12.

Poese, M.E., and Garrett, S.L. (2000) 'Performance measurements on a thermoacoustic refrigerator driven at high amplitudes', *J. Acous. Soc. Am.* vol. 107, pp. 2480-2486.

Rott, N. (1980) 'Thermoacoustics', *Adv. Appl. Math.* vol. 20, no. 135.

Sun, D., Qiu, L., Zhang, W., Yan, W., and Chen, G. (2005) 'Investigation on travelling wave thermoacoustic heat engine with high pressure amplitude', *Energy Conversion and Management*, vol. 46, pp. 281-291.

Swift, G.W. (1988) 'Thermoacoustic engines', *J. Acoust. Soc. Am.* vol. 84, pp. 1145-1180.

Swift, G.W. (1992) 'Analysis and performance of a large thermoacoustic engine', *J. Acoust. Soc. Am.* vol. 92, pp. 1551-1563.

Swift, G.W. (2002) *Thermoacoustics: A unifying perspective for some engines and refrigerators*. Acoustical Society of America, New York, NY.

Tang, K., Chen, G.B., Jin, T., Bao, R., Kong, B., and Qiu, L.M. (2005) 'Influence of resonance tube length on performance of thermoacoustically driven pulse tube refrigerator', *Cryogenics*, vol. 45, pp. 185-191.

Tijani, M.E.H. (2001) *Loudspeaker-driven thermo-acoustic refrigeration*, PhD thesis, Eindhoven University of Technology.

Tijani, M.E.H., Zeegers, J.C.H., and de Waele, A.T.A.M. (2002a) 'Construction and performance of a thermoacoustic refrigerator', *Cryongenics*, vol. 42, pp. 59-66.

Tijani, M.E.H., Zeegers, J.C.H., and de Waele, A.T.A.M. (2002b) 'Design of thermoacoustic refrigerators', *Cryogenics*, vol. 42, pp. 49-57.

Ueda, Y., Biwa, T., Mizutani, U., and Yazaki, T. (2004) 'Experimental studies of a thermoacoustic Stirling prime mover and its application to a cooler', *J. Acoust. Soc. Am.*, vol. 115, no. 1134-1141.

Ward, W.C., and Swift, G.W. (2001) *Design Environment for Low-Amplitude ThermoAcoustic Engines (DeltaE) Tutorial and User's Guide (Version 5.1)*. Los Alamos National Laboratory, New Mexico.

Wetzel, M., and Herman, C. (1997) 'Design optimisation of thermoacoustic refrigerators', *Int. J. Refrig.*, vol. 20, no. 1: pp. 3-21.

Wollan, J.J., Swift, G.W., Backhaus, S., and Gardner, D.L. (2002) 'Development of a thermoacoustic natural gas liquefier', *AIChE New Orleans Meeting*, New Orleans LA.